This is shown by direct measurements of length and by observing the changes in orientation (inclinations of up to 30° were observed for the cubic fracture plane). The same applies to crystals wetted without load (cf. Fig. 195). Extension occurs also in specimens with the axis parallel to one of the body diagonals, but on a smaller scale, presumably by cubic glide [(551), (552), (554)]. The fractured rods can be more easily coloured by ultra-violet light as a consequence of the preceding deformation (556). A tensile test in which the load is increased rapidly with the object of minimizing extension so far as possible is described in (548).

4. Tempered crystals whose strength in the dry state had been reduced almost by half, attain in the Joffé tensile test the same high

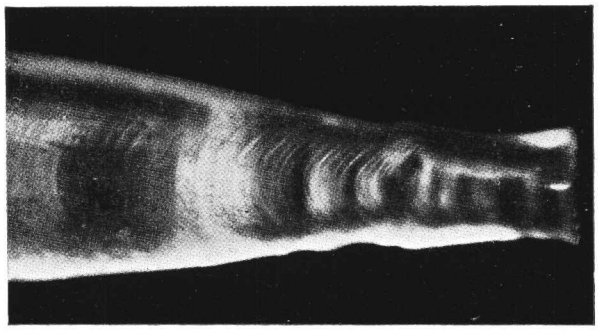

FIG. 195.—Glide Bands on a Wetted NaCl Crystal without Load after Subsequent Fracture in the Dry State (551).

values as are exhibited by material which has not been previously treated [(551), (552)].

5. High tensile strengths are exhibited by rock salt crystals even when dissolved in more or less saturated solutions of NaCl (investigated in up to 80 per cent. saturated solutions) [(551), (559)]. The effect is said to be absent if the solution is saturated (546). The same mechanical properties as in water were also obtained in concentrated sulphuric acid and in a 25 per cent. solution of SO_3 in H_2SO_4 in which NaCl is decomposed (557).

6. The Joffé effect was found with crystals of potassium chloride and potassium iodide immersed in water, and with potassium iodide immersed in anhydrous methyl alcohol [(558), (557)].

There is still some uncertainty as to the relation between the increase of strength on the one hand, and the initial stress, degree of solution and the deformation which precedes fracture, on the other.

The experimental results differ in regard to the after-effect of solution. Whereas in the bending test the increase in plasticity ceases as soon as the water is removed (547), in the tensile test the normal strength of the dry state is not regained until after a few days (548). The time required for this after-effect varies with the solvent (559).

With NaCl specimens oriented parallel to the cube edge it is very noticeable that down to a definite initial stress of 216 g./mm.^{2} no increase in strength takes place (551). In this case the crystals do not fracture where the cross-section is smallest, but in the zone that has remained dry, about 0·1–0·5 mm. above the water level. The tensile values are therefore identical with the initial stress, which is about 50 per cent. lower than the normal dry strength. These tests give no indication as to the strength of the portion which has been exposed to the solvent. Where the initial stresses are small there is appreciable solution, fracture takes place in general at the narrowest part of the crystal, and high tensile strengths are obtained. Dependence of the strength upon the magnitude of the applied stress, if it exists at all within this range of initial stress, merely takes the form of a slight increase of strength as the initial stress is reduced. Complete independence of the initial stress would involve the independence of the resultant strength from the degree of solution. This conclusion is not borne out by the tests carried out with wetted specimens under no load, mentioned under (1).

Owing to the shape of the wetted crystals the recognition of a relationship between the increased tensile strength and previous deformation is difficult (cf. Fig. 194). The extension is by no means distributed evenly over the wetted portion of the crystal. In any case, so far all tests devised to reveal a clear connection between strength and the degree of deformation have failed. Even specimens with axis parallel to a body diagonal show the same increase in strength, although the extension is very slight.

There is still no satisfactory explanation of the solution effect. The explanations attempted hitherto differ in their basic assumptions.

According to the interpretation suggested by the discoverer of the effect, the cause of the increase of strength is to be sought in the elimination of surface cracks which, by their notch effect, tend to lower the strength (546). The inherent strength of the *crystal* is not raised; the *technical* strength obtained in the normal tensile test is less than that of the true strength of the crystal owing to the notch effect of the fine cracks which are always present. In support of the view that stresses of the order of 100 kg./mm.^{2} can actually

occur in the interior of crystals, tests have been carried out with spheres of rock salt whose temperature had been suddenly raised from the temperature of liquid air (560). The stress produced within the specimen on immersion in a lead bath at 600° C., which was calculated at 70 kg./mm.^{2} and which did not lead to fracture, was regarded as a confirmation of the high inherent strength of the crystal.

An objection to this interpretation is that it assumes a very great depth for the surface cracks, since no increase in strength is produced until a large part (more than 50 per cent.) of the section has been removed. The " sphere " experiment has also been objected to on the grounds that plastic deformation occurs in the surface layers, thus preventing the development of high stresses in the interior (561).

Recently this view has been discussed again with the necessary addition that the depth of the crack depends on the dimensions of the crystal (562); in this way an explanation can also be found for the increase of strength observed with very thin crystals in the dry test (563).

According to a second explanation of the Joffé effect, the increase in strength is to be ascribed to the preceding deformation. It is assumed that the strength of the undeformed crystal is small and that it rises only as a result of deformation to the high values which are theoretically required (561). The effect of the water is believed to consist in the removal of impediments from the surface, thus assisting the crystal to deform (547).

This interpretation assumes the existence of a definite relationship between the observed strength and the degree of deformation which, however, has so far not been proved. In this connection attention is again drawn to the results which were obtained with specimens parallel to the body diagonals and which are difficult to reconcile with this assumption.

A combination of the two conceptions is discussed briefly in (553), (564). The high strength is attributed exclusively to the effects of work hardening. The requisite high degree of plasticity exhibited by the wetted crystals is believed to be due to the removal by solution of cracks which develop in the course of gliding, and which in the dry test lead to fracture.

Further attempts at elucidation assume that water penetrates into the crystal. While on the one hand the crystal is presumed to acquire in this way a very great capacity for strain strengthening (" *Reissverfestigung* ") (565), it is also believed, especially in view of experiments on the dependence of the Joffé effect upon orientation,

that changes in the interior of the crystal due to the penetration of water are mainly responsible for the high strengths obtained (551). That plastic deformation is not an indispensable condition for the change in the mechanical properties of wetted crystals is suggested by the increased scratch hardness of crystals subjected to extensive solution (566); however, in later tests in which solution was less severe this increase was not found (567). An increase in the ionic conductivity also points to an internal effect of the water (565).

Although it was not possible to obtain a direct verification of the penetration of the water by measuring the lattice constants and the density [with an accuracy of about 0·1 per thousand (566)], this proof has been supplied for wetted crystals by observing in them the ultra-red absorption typical of water (568).

With the object of disproving the theory that penetrating water is responsible for the increase in strength, experiments were carried out in which narrow strips of crystal were protected against solution by a coating of vaseline; the observed strengths agreed with those obtained in the dry test (569).

From what has been said it will be seen that a satisfactory explanation of the Joffé effect has still to be found. An important contribution to the solution of this problem would probably result from tensile tests carried out on crystals in varying stages of dissolution, and in which plastic deformation during the tests had been minimized (low temperature, short distance between the clamps).

CHAPTER VIII

THEORIES OF CRYSTAL PLASTICITY AND CRYSTAL STRENGTH

The deformation and fracture of crystals obeys a number of laws. Although the criterion of mechanical twinning has not yet been established, the most important of the deformation mechanisms (gliding) has already been largely elucidated. The principal facts are given in Section 50; they can be recapitulated as follows:

1. Shear stress law.
2. Low critical shear stress which, down to the lowest temperatures, is only slightly dependent on temperature.
3. Increase in the shear strength with increasing glide; work hardening.
4. Dependence of work hardening on temperature (and speed of deformation). This is insignificant at the lowest temperatures and close to the melting point, but substantial at intermediate temperatures.

A simple law has also been discovered governing the cleavage fracture of crystals (Sohncke's normal stress law). The values for the critical normal stresses are as low as for the critical shear stresses for glide.

A physical theory should have for its object the formulation of a conception of the structure of the solid which explains the empirical laws, and the quantitative derivation therefrom of the observed values of the mechanical properties. In addition, the processes of recovery and recrystallization which are observed in plastically deformed crystals (Section 49 and Chapter VI, G) have also to be explained.

It is naturally a condition of the theoretical interpretation of the tensile and shear strengths of crystals that the effective binding forces and the laws by which they are governed should be known. It is precisely in this field, however, that our knowledge is limited. According to whether the lattice particles are ions, or atoms showing no polarity, a distinction is made between polar and non-polar binding. Theoretically the position is clearest in the case of the polar (heteropolar) crystals, such as salts. Here electrostatic

forces are responsible for holding the lattice together; the law assumed for these has been generally confirmed. To the crystals of non-polar binding belong, first of all, the metals. According to present conceptions a metal crystal is held together by positively charged atom cores embedded between the free metal electrons. However, there is still no satisfactory theory on the subject.[1] Other non-polar crystals are the molecule lattices (H_2,N_2,CO and many organic compounds) and the crystals of the rare gases. In this case it has been possible, with the aid of quantum mechanics, to account for the attractive forces which hold the lattice together by attributing them to the deformability of the molecules or atoms. The forces decrease with the inverse seventh power of the distance. Special difficulties arise with a series of non-polar crystals, such as materials of the diamond type with tetrahedral bonds, benzene, etc.

73. *Theoretical Tensile Strength*

The mechanical property which, so far, has been examined theoretically in greatest detail is the tensile strength. The only calculations carried out strictly on the basis of the lattice theory relate to the tensile strength of rock salt, that is of an ionic crystal. This is because the ionic crystals best illustrate the laws of the interatomic forces. Two forces are mainly effective in these heteropolar crystals: electrostatic (Coulomb) forces between the ions, and a repulsive force which prevents the ions from penetrating into each other. The electrostatic forces are governed by Coulomb's law, repulsion by the interaction of the electron clouds of the ions. In view of the existence of a stable equilibrium, repulsion is bound to diminish much more rapidly with the distance than the attraction. At a given distance, represented by the lattice constant, attraction and repulsion are in equilibrium. From this we obtain for the force (K) the equation (570)—

$$K = \frac{e^2}{\rho^2} - \frac{b}{\rho^n + 1} \cdot \quad . \quad . \quad . \quad . \quad . \quad (73/1)$$

in which e and ρ represent the charge and the distance between the ions, while b and n are constants (cf. Fig. 196). $n \simeq 9$ was determined for the alkali halides from the lattice constants and the compressibilities. In order to arrive at the tensile strength it is necessary to know also the "lattice energy" ϕ, *i.e.*, the energy which must be employed in order to dissociate completely 1 g.

[1] *Translator's Note.* This statement is no longer true: see the works of Mott and Jones, Brouillin, Seitz, Hume-Rothery and others.

molecule of the crystal (to place infinite distance between the ions).

If now a crystal of rock salt is stressed parallel to a cube axis, then the cubic lattice (with the lattice constants, a_0) is transformed into a tetragonal lattice (with the constants a and h). In this

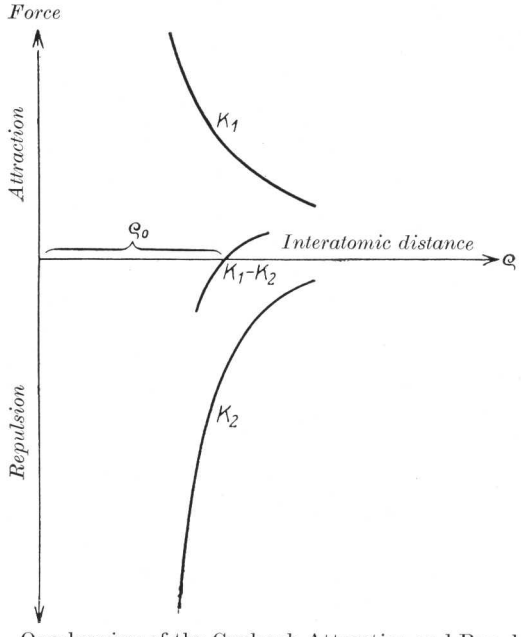

FIG. 196.—Overlapping of the Coulomb Attractive and Repulsive Forces in Ionic Crystals.

process, of course, the lattice energy of the crystal depends on h. But since Poisson's ratio results solely from elongation, then

$$\left(\frac{\partial\phi(a,\,h)}{\partial a}\right)_h = 0$$

from which the functional connection of a and h is obtained. If inserted in the expression for ϕ, then the lattice energy is obtained solely as a function of h. If the tensile stress K is necessary in order to increase h by dh, then clearly $K \,.\, dh$ is equal to the reduction of the lattice energy $d\phi$:

$$K = -\frac{d\phi}{dh}. \quad . \quad . \quad . \quad . \quad . \quad (73/2)$$

If h increases from a_0 onwards, then initially the repulsive force increases also in an attempt to restore the original undeformed

condition. This increase in strength, however, does not persist at greater deformations. After a maximum has been exceeded the energy soon becomes negligibly small as dilatation continues. The maximum K_z corresponds to the tensile strength. It can be calculated from (73/2) for a constant h characterized by $\frac{d^2\phi}{dh^2} = 0$. The calculated tensile strength for cubic specimens of rock salt (571) was 200 kg./mm.^{2} with an elastic elongation of 14 per cent.[1] Similar elongations before fracture are also to be expected for other ionic crystals, so that about one-tenth of the modulus of elasticity in the direction of stress may be regarded as a rough indication of the theoretical tensile strength.

The same order of magnitude for the tensile strength of crystals was derived from energy considerations (573) which, owing to their independence of the valid law of energy, are by no means limited to ionic crystals. The basic idea is as follows. The additional surface energy which results from the development of the two fracture planes must at the moment of fracture be available in the crystal as elastic energy of deformation. In order that the surface energy may be fully effective, it is necessary that the distance between the two fracture planes shall be greater than the range of action of the molecular forces. Let Δl be the elastic extension of the specimen immediately prior to fracture. If the grips are held rigidly in position, this amount is also the distance between the two fracture planes. If now α is the free surface energy and Z the tensile strength, then

$$Z \,.\, \Delta l > 2\alpha \quad . \quad . \quad . \quad . \quad . \quad (73/3)$$

since the elastic stress energy is certainly smaller than $Z \,.\, \Delta l$. With the aid of the values for α and Z it is therefore possible to calculate a lower limit for the range of molecular forces. For rock salt (α NaCl $\sim$ 150 dyn/cm., $Z = 2{\cdot}2 \,.\, 10^7$ dyn/cm.^{2} for fused crystals) the value is $\sim$1400 Å. Undoubtedly this value is unduly large since we know from other sources that the radius of action of the lattice forces is no greater than the distance between the lattice points (amounting to a few Å.). This contradiction could be resolved only by assuming a tensile strength which was 100–1000 times greater than that experimentally determined.

[1] Recently in place of (73/1) a law of energy was quoted in which repulsion is represented by an experimental function and in which allowance is made for the van der Waals forces of attraction which are always present (572). A new calculation of tensile strength has not yet been undertaken. It is true, however, that the lattice energy will vary by no more than 0·2 per cent. if rock salt is used.

If this method of estimating the theoretical tensile strength is applied to metallic crystals, values are obtained which again exceed the test values by many orders of magnitude. In zinc crystals, for instance, Δl is $\sim$9000 Å. when fracturing about a basal plane disposed obliquely to the tensile direction ($a_{Zn\ \text{fused}} \sim 800$ dyn/cm.* $Z_{(0001)} = 1{\cdot}8 \cdot 10^7$ dyn/cm.^{2}).

The main conclusion to be drawn from these considerations is that the observed tensile strengths of crystals cannot be regarded as due to a breakdown of the lattice forces over the whole of the fracture area. The lattice strengths are higher than the technical strengths by 2–3 orders of magnitude. Independently of any calculation this is readily shown by the fact that the modulus of elasticity is constant nearly to the point of fracture (574). If the forces which hold the crystal together were, in fact, overcome at the moment of fracture, then this would correspond to a modulus of elasticity of zero, parallel to the tensile direction, and thus appreciable reductions in the modulus should be observed at an earlier stage.

74. *Calculations of the Theoretical Shear Strength*

The conception underlying a (lattice) theoretical calculation of the shear strength of glide planes is that the forces which are effective between the lattice planes can be represented by a model resembling a file (575). A reciprocal displacement in a longitudinal direction of two files in direct contact is possible only if they are slightly separated from each other before each stage of glide begins. Normal dilatation perpendicular to the glide planes is also stated to be a condition of glide in crystals. Before glide can take place, therefore, it is necessary to reduce the cohesive forces. A mathematical analysis of this model in terms of the lattice, making certain assumptions for the sake of simplicity, gives the same order of magnitude for the relationship between shear strength and shear modulus (1 : 10) as was found above for the relationship between tensile strength and modulus of elasticity. Just as the elastic extension should amount to about 10 per cent. at the point of fracture, so, too, the elastic shear should be about 10 per cent. at the start of glide. The theoretical shear strengths, like the tensile strengths, amount to several hundred kg./mm.^{2}. This gives for the magnitude of normal dilatation perpendicular to the glide plane a value of 1–2 per

* The (unknown) surface energy of the crystal is greater; it implies therefore an even greater value of Δl.

cent. of the tangential displacement. Fig. 197 shows clearly that glide cannot proceed along these lines. It shows the movement perpendicular to the glide plane which is exhibited at the yield point by zinc crystals of various orientations. Whereas normal *dilatation* occurs when the basal plane makes a large angle with the crystal axis, glide is accompanied by normal *contraction* where the initial position of the basal plane in relation to the longitudinal direction exceeds 27° 30′.

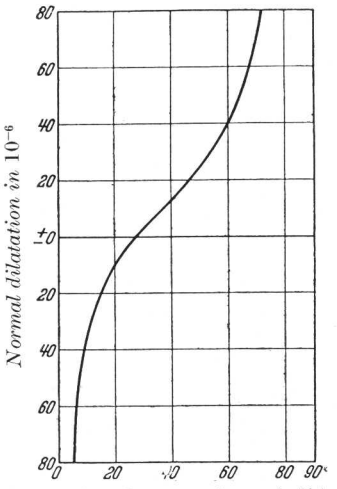

FIG. 197.—Normal Dilatation (ϵ_z) Perpendicular to the Glide Plane at the Yield Point of Zn Crystals.

$$\epsilon_z = S_{33} \operatorname{tg} \chi + S_{13} \operatorname{cotg} \chi.$$

The same order of magnitude for the theoretical shear strength of glide systems is derived from a rough estimate which assumes that the two halves of a crystal would have to be elastically displaced with reference to each other by about half a glide unit, if they are to pass into the new position without additional stress (576).

Actual shear stress values are smaller than these high values by more than three orders of magnitude (about 100 g./mm.^{2}). Here, too, then, the lattice forces are by no means overcome—a fact which appears clearly from the low shear values (about 10^{-4}) which prevail at the yield point. Just as crystals fracture long before the tensile strength of the lattice is reached, so, too, glide, and probably mechanical twinning, occur long before the shear strength of the lattice is attained.

75. *Attempts to Resolve the Difference between the Theoretical and Technical Values*

Although it is generally impossible to realize in practice the tensile shear strengths which have been determined theoretically, it is, nevertheless, quite obvious that the lattice strengths must exceed the experimental values by several orders of magnitude. The failure of the crystals under mechanical stressing (start of gliding and twinning; fracture) is premature and takes place long before the lattice forces have been overcome. In an attempt to account for this great difference, Voigt drew attention to the significance of structural and thermal inhomogeneities in the actual crystals (577).

Both of these ideas have been further developed. The structural inhomogeneities provide the basis of Smekal's theory of vacant lattice sites [(578), (579)]. According to this theory, real crystals differ fundamentally from the ideal crystal by reason of the defects in their lattice (holes, defective orientation, foreign atoms). In the case of transparent crystals these defects can be experimentally demonstrated in a number of ways (*e.g.*, coloration, absorption). Some idea of the prevalence of lattice faults can be gained from an estimate which gives one fault for every 10,000 atoms built perfectly into the lattice. Since the faults originate while the crystal is growing, their frequency and their nature depend both on the material itself and on the conditions under which it crystallizes. The properties of the crystal which are decisively influenced by these faults (the structurally sensitive properties) contrast with the structurally insensitive properties which in the main are determined by the ideal lattice units distributed between the faults (cf. Section 60).

The significance of the faults in the lattice for bridging the large gap between technical and lattice strengths is to be sought in their notch effect. This is due to the fact that, when cracks are present in an elastically stretched solid, appreciable changes in the stress distribution will occur in the vicinity of the cracks. Initially, elastic deformation will increase with stress, yet only up to the point at which either the maximum stress achieved is equal to the lattice strength, or until less energy is required (surface energy) to enlarge the crack than to increase the stress. The stress attained at this point represents the technical tensile strength.

In the case of a plate with an elliptical hole (radii a and b) which is subjected to a tensile stress σ in the undisturbed zone, in the plane perpendicular to the major axis, a maximum stress will occur at the edge of the hole

$$\sigma_{\max.} = \sigma\left(1 + \frac{2a}{b}\right) \quad . \quad . \quad . \quad . \quad (75/1)$$

at the ends of the major axis, while at the ends of the minor axis there will be a compression stress of $-\sigma$ (580). If $\left(\rho = \frac{b^2}{a}\right)$ represents the radius of curvature at the apex of the ellipse, then the expression for the maximum stress becomes

$$\sigma_{\max.} = \sigma\sqrt{\frac{a}{\rho}} \quad . \quad . \quad . \quad . \quad . \quad (75/1a)$$

In order to calculate, on an energy basis, the technical strength

required to extend a crack, it is first necessary to ascertain the elastic energy inherent in a thin plate containing a slot (581). It will be found that in a plate (thickness I) subjected to stress σ the stored elastic energy is less by

$$A_e = \frac{I}{E}\pi a^2\sigma^2$$

(E = modulus of elasticity, a = half the length of the slot) than in a plate that is intact. Also there is in the plate with the crack an amount of energy equal to $4a\alpha$ (α = surface energy) which originates from the surfaces of the crack. Fracture of the crystal will occur without the addition of further energy if the elastic energy which has been acquired by widening the crack just suffices to supply the surface energy needed to enlarge the surface. Therefore

$$\frac{\partial}{\partial a}\left(\frac{I}{E}\pi a^2\sigma^2\right) = \frac{\partial}{\partial a}(4a\alpha)$$

is the equation for determining the tensile strength σ_1; it results in the expression

$$\sigma_1 = \sqrt{\frac{2E\alpha}{\pi a}} \quad . \quad . \quad . \quad . \quad . \quad (75/2)$$

by means of which the tensile strength of an elastic solid can be calculated from its shape, that is, from the length of the existing cracks and from its physical properties. This theory has been tested and confirmed on scratched glass and quartz.

The notch effect associated with the microscopic cracks discussed above is also influenced by the faults in the crystal referred to earlier in this section. With the aid of the formula (75/2), and if the tensile strength, modulus of elasticity and surface energy are known, then a length of crack corresponding to the faults can be calculated (582). For example, the following values were obtained for rock salt and zinc: rock salt ($\sigma_1 = 2{\cdot}2 \cdot 10^7$ dyn/cm.^{2}; $\alpha = 150$ dyn/cm.; $E = 4{\cdot}9 \cdot 10^{11}$ dyn/cm.^{2}) $2a = 0{\cdot}2$ cm.; zinc (fracture along the basal plane; $\sigma = 1{\cdot}8 \cdot 10^7$ dyn/cm.^{2}; $\alpha = 800$ dyn/cm.; $E = 3{\cdot}5 \cdot 10^{11}$ dyn/cm.^{2}) $2a = 1{\cdot}1$ cm. Naturally, no real significance attaches to such large cracks. Formula (75/2), of course, can be used only if the maximum tensile stresses at the edge of the notch do not exceed the strength of the lattice. But for the cracks whose lengths have already been obtained from the plausible assumption that the radius of curvature at the base of the notch is of the same order of magnitude as the lattice constants ($5 \cdot 10^{-8}$ cm.), this has already occurred. (75/1a) gives for rock salt $\sigma_{max.} = 630$ kg./mm.^{2},

for zinc $\sigma_{max.} = 1200$ kg./mm.^{2}, which values are about three times higher than the lattice strengths recorded in Section 73. (75/1*a*) shows that cracks ten times as short would suffice to overcome the lattice strength at the base of the notch. Even in that case, however, the cracks would still be of macroscopic dimensions, which is contrary to the prevailing conception of the nature of a fault in a crystal. An attempt to postulate even shorter cracks with the aid of plastic glide will be found in (583).

Although we have been unable to account quantitatively for the low mechanical properties of crystals along these lines, qualitatively the concept employed leads to a plausible interpretation of a series of phenomena (578). The selection of fracture planes would be decisively influenced by the spatial distribution of crystal faults, for instance, along planes of minimum surface energy. The Sohncke normal stress law is derived from the fact that the maximum stress at the base of the notch results from the stress components perpendicular to the crack. Likewise the small effect of temperature on the critical normal stress is also explained. Further, the increase in the tensile strength of polycrystalline specimens with decreasing grain size (582) has been accounted for by assuming that the cracks are halted initially at the grain boundaries and do not penetrate into the adjacent grain until the external stresses have been increased (584). In order to avoid the long cracks which, in thin crystals at least, are obviously impossible, attention has been drawn on the one hand to the reciprocal intensifying effect of neighbouring cracks (578). On the other hand, it was assumed (cf. Section 72) that the crack length ceases to be a constant of the material if the dimensions of the solid come within its order of magnitude (584).

The effect of surface cracks on the tensile strength of mica sheets is made very clear in (585). By removing the load from the edges of the specimens (the width of the specimens was greater than the width of the grips) the tensile strength was increased tenfold. Consequently, it amounted to about one-tenth of the theoretical value, which shows that in this instance the effect of *internal* faults was no longer decisive. This can be explained in terms of the notch theory by assuming that, in the mica under investigation, the structural faults were disposed mainly parallel to the cleavage plane, *i.e.*, parallel to the direction of pull.

It was only natural that the notch effect of cracks and faults should be adduced to account also for the low shear strength of crystals. To facilitate calculation an extended ellipse was again substituted for the crack, the stress distribution being determined

along the boundary of the ellipse [(586), (587)]. The result is wholly in line with that obtained in the tensile test. The decisive factors are the length of the crack and the radius of curvature at its end. Stress concentration again occurs at the ends, and the direction of maximum shear stress coincides with the direction of the crack itself. In spite of lower total effective shear stress, it is there that the shear stress of the lattice is said to be reached and that glide begins. According to this conception, therefore, the glide elements of the crystals would be decisively influenced not only by the anisotropy of the lattice strength but also by the distribution of the faults.[1]

The formula for the shear strength τ_1, which, like formula (75/2), is obtained by balancing the energy, is as follows :

$$\tau_1 = 2\sqrt{\frac{G \cdot \alpha}{\pi a(1-\mu)}} \quad . \quad . \quad . \quad . \quad (75/3)$$

in which G represents the modulus of shear and μ Poisson's ratio (587). Cracks of the same order of magnitude as those which have already been derived from the formula for tensile strength are obtained.

A theory which avoids these large cracks can be developed if the following conception of the mechanism of glide is adopted (589). Glide starts locally at random points in the crystal as a result of " dislocations " (deviations from the strictly geometrical lattice structure; caused probably by thermal movement) which become separated from each other, under the influence of the local shear stress, by migration parallel to the direction of gliding. In the ideal crystal the migration of the first few " dislocations ", or in other words the plastic deformation, would begin at minimum shear stresses. It is fundamental to this theory that these dislocations do not migrate through the whole crystal, but very soon meet with obstacles which prevent them from scattering beyond a mean distance L. It is mainly from this picture that the slope of the hardening curve is derived. From a comparison between observed and calculated curves a value of about 10^{-4} cm. is obtained for the length L.

In order to explain the experimentally determined final values for yield point, reference is made to the mosaic structure which is

[1] The *weakening* effect of the notches described above has nothing to do with the shear *hardening* which is produced in plastic crystals by subsequently perforating or notching them (Fig. 198). In this case it is a question of producing lattice disturbances which impede glide in the vicinity of the notches.

often observed in natural crystals. The crystal is composed of lattice blocks, having roughly the same linear dimensions as L, which are rotated from each other about small angles of approximately 1′ (590). In consequence, internal stresses develop within the crystal. An estimate gives shear stresses approximately one ten-thousandth of the shear modulus. Not until these stress limits have been overcome can the dislocations start to migrate in the crystal mosaic, and plastic strain occur. It will be seen that the order of magnitude of the experimentally determined critical shear stresses has in this way been correctly given.

Dislocations are also assumed to be nuclear points of glide in (591) and in (592) (in the former they are illustrated by the picture of a vernier).

Hitherto, low strength was always attributed to faults which, while their orientation corresponds to the anisotropy of the crystal, are statistically distributed throughout it. A theory of a more sweeping nature assumes the existence of regularly distributed

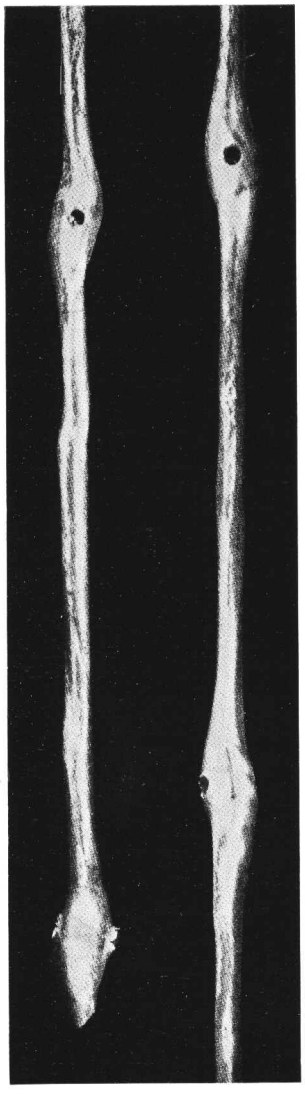

(*a*) Tensile specimens of a perforated Mg crystal.

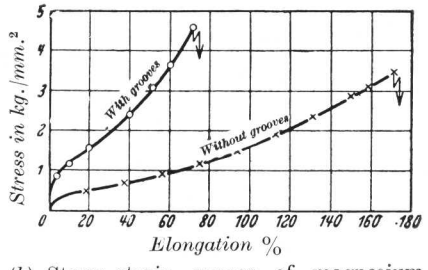

(*b*) Stress–strain curves of magnesium crystals with and without longitudinal grooves.

Fig. 198 (*a*) and (*b*).—Shear Hardening of a Crystal Caused by Subsequent Drilling and Notching (588).

inhomogeneities, and connects these with a reduction in the potential energy of the crystal and consequently with the creation of a more stable condition than that represented by the normal lattice (593). The normal lattice structure is said to be overlaid by a " secondary " structure, characterized by the periodical occurrence, at distances of a multiple of the lattice constants, of planes which are abnormally close packed. According to (594), (595), however, the calculation carried out for the crystals of alkali halides cannot be regarded as valid for a less symmetrical lattice of higher stability. Consequently, although there is much experimental data to support the theory of the construction of actual crystals from the lattice blocks, it is unlikely that an explanation along these lines will be possible. Moreover, it has been shown that the mosaic texture is not a general but an individual property which is appreciably dependent on the conditions of growth and deformation (596). How far this applies to the adsorption of small additions into the internal surfaces of crystals [for ionic crystals cf. (597); for Bi (598)] cannot yet be decided. An attempt to account for the great difference between the theoretical and experimental values on the basis of a secondary structure would therefore appear to be inadmissible.

In this connection, attention is drawn to the very different function performed by the system of internal surfaces in the glide theory based on the migration of " dislocations " which has been outlined above. In this theory the " dislocations " serve solely to restrict migration; the process of deformation takes place in the interior of the blocks.

The theories we have been discussing assume that structural inhomogeneities are the cause of the premature failure of actual crystals. The second type of inhomogeneity to which reference has already been made, namely thermal, originates in the thermal movement of the atoms. Becker has very carefully studied their effect on glide [(599), (600)]. In this case, however, it was not, as hitherto, the onset of plastic flow that was calculated, but the speed of flow (u) as a function of the applied shear stress (S) and of the absolute temperature (T). The line of thought is roughly as follows: irregular thermal movement in the neighbourhood of the glide planes causes stress fluctuations to be superimposed on the applied shear stress. After short periods the shear stress increases to the value of the lattice shear strength (S^*): the crystal glides by discreet amounts. The increase in length of the crystal per second (the speed of flow) is obtained from the product of Z, the number of

glide-plane sections involved in a unit of glide, the average length Δl by which the specimen is extended as a result of such a unit of glide and the probability W that such glide will occur :

$$u = Z \,.\, \Delta l \,.\, W \quad . \quad . \quad . \quad . \quad . \quad (75/4)$$

For the probability W, *i.e.*, the frequency with which the limiting stress S^* is exceeded in the vicinity of the glide plane, within a volume V we obtain

$$W = e - \frac{V(S^* - S)^2}{2GkT} \,. \quad . \quad . \quad . \quad (75/4a)$$

in which G represents the modulus of shear and k the Boltzmann constant ($1{\cdot}37_2 \,.\, 10^{16}$ erg/degree). In experiments with tungsten crystals (599) and polycrystalline copper (601) the marked dependence of the speed of flow upon temperature (the speed being doubled when temperature rises by 10°), which follows from formula (75/4), was very well confirmed.

However, an attempt to account for the low experimental shear strengths exclusively in terms of thermal fluctuations meets with difficulties owing to the low values for critical shear stress which have also been observed at very low temperatures. The observed dependence of the flow speed upon temperature can also be regarded as an effect of crystal recovery, which works in opposition to the work hardening which accompanies increasing deformation (Section 49). Since recovery depends on the effect of thermal fluctuations (cf. Section 77), it should be easy to interpret the results of the flow experiments (576). On the other hand, in the case of the amorphous solids, plasticity seems, in fact, to result exclusively from thermal fluctuations (cf. also Section 77).

In (592) the effects of both structural and thermal inhomogeneities are combined to explain the low shear stresses of crystals. Notches are held mainly responsible for the wide discrepancy between theoretical and experimental shear strengths; they cause stress concentrations amounting to about one-third of the theoretical shear strength. Nevertheless, thermal fluctuations are said to impose characteristic features on crystal glide. If certain allowances are made, the slight dependence of the critical shear stress of zinc and cadmium crystals upon temperature also agrees in general with the theory. On the other hand, the marked dependence upon temperature of the flow speed of these metals, on which the application of the thermal theory rests, has still to be proved.

76. *Theory of the Work Hardening of Crystals*

It has been shown that so far no reliable explanation of the low tensile and shear strength of crystals has been forthcoming. Even less is known of the phenomenon of work hardening, which consists in an increase in the mechanical properties with increasing deformation. This subject still remains within the realm of speculation.

Recent theories of the notch effect naturally assume that hardening results from changes in the strength-reducing notches. The shear and tensile strengths of the lattice are assumed to be fixed; the experimentally determined values can only approximate to them; they can never exceed the lattice strength; a hardening of the lattice is impossible. Several opinions have been expressed as to the kind of changes which must occur in the notches in order to reduce their effect. For instance, as a result of deformation, the cracks associated with the faults in the structure of the crystal could be shortened. It is therefore reasonable to suppose that the dangers to which they give rise are reduced, where simple glide is involved, for the *latent* planes, while in the case of complex glide the relief is more general. Owing to the movement of the glide "packets" the cracks are further subdivided, and the individual portions displaced stepwise in relation to each other (584). The relatively slight changes in the tensile strength of metals with unique glide planes (Sections 53 and 54) are also in agreement with this conception. In regard to the shear hardening of the *operative* glide plane, it has been pointed out that glide occurs at an increasing number of points as deformation proceeds. Whereas the stress concentration at the ends of the cracks which first become effective is very high, by reason of the fact that the load has been removed from large areas in the vicinity, the areas which remain undeformed diminish as elongation proceeds. In terms of the notch-effect theory it follows that the new cracks must be increasingly short, and their stress concentration correspondingly low: thus, the glide plane hardens (586). According to the more recent conception of glide as a migration of dislocations (589) the shear hardening is similarly interpreted as an increase in the number of dislocations. As the distance between the dislocations is reduced (perpendicular to the plane of gliding) the shear strength increases. This theory yields the following expression for the connection between shear strength (S) and gliding (a), *i.e.*, for the shear-hardening curve

$$S = \kappa \,.\, G\sqrt{\lambda/L} \,.\, \sqrt{a} \quad . \quad . \quad . \quad . \quad (76/1)$$

in which G represents the modulus of shear, λ the identity period

in the glide direction, L the distance of the free migration of the dislocations (size of the lattice blocks; approx. 10^{-4} cm.) and κ a constant (approx. 0·2). The shear-hardening curves are thus represented by parabolas, and there is, in fact, close agreement with the experimental results obtained with cubic metals.

In this connection mention must be made of a theory which associates strain hardening with increasing disorientation along the glide planes (578). This is related to the rotation of portions of the lattice in the vicinity of the glide planes (cf. Section 59), which has been theoretically deduced and experimentally demonstrated from the stress distribution at the crack [(587), (586)]. As strain along the operative glide planes is intensified the single crystal is said to disintegrate into lattice blocks of increasingly variable orientation. This not only impedes further glide (shear hardening), but it also renders more difficult the formation of smooth fracture planes permeating the entire crystal (tensile hardening). It should be noted, however, that if the direction of stress is reversed the degree of disorientation will be reduced, but the hardening will continue to increase (cf. Sections 59 and 61).

The hypotheses of the nature of work hardening so far described relate to changes which take place, during gliding, in the strength-reducing faults present in the crystal. The tendency of these changes is to increase the effective lattice strength with the percentage of working. According to other hypotheses, which take no account of the discrepancy between the theoretical and actual strengths of crystals, the phenomenon of hardening is due to modifications of the crystal lattice. These include the earlier modification hypotheses, together with the version in which they are best known: the amorphous layer hypothesis [(602), (603)] which assumes the formation of a brittle and amorphous layer between the gliding lamellæ, and at the grain boundaries, as a result of friction. Apart from the fact that no proof could be adduced for the occurrence of such layers, there are thermodynamic grounds for rejecting this assumption (604). In this context mention should also be made of the displacement hypothesis (experimentally disproved) (605), which assumes a lattice displacement, to the point of complete destruction, in the course of deformation.

According to the interference hypothesis (606) *local* disturbances of the crystal lattice, and consequently of the interatomic forces, are regarded not only as an important cause of hardening by cold working, but also of hardening through alloying. A more precise picture of local lattice disturbances of this type is obtained if the

glide lamellæ are visualized as being elastically bent (Fig. 199). In the case of glide accompanied by bending [(607) and especially (608)] the lamellæ are not displaced parallel to each other; instead, in the course of gliding they curve about an axis which in the glide plane is perpendicular to the glide direction. Compared with its original intact condition, the lattice in the bent crystal is changed. In the first place the boundary planes of the bent lamellæ represent "internal separation planes", while, secondly, elastic stresses (tensile or compressive stresses on the convex or concave side of the lamellæ) are distributed inhomogeneously in the crystal. In the present case the model of the macroscopically bent crystal does not limit application of the general theory, since undulations of the glide planes have also been determined by X-ray diffraction in crystals which have been extended uniformly. Hardening, especially hardening of the latent glide systems, is now attributed to the internal separation planes. These prevent glide planes which intersect the first planes from becoming effective. Hardening of the primary system, together with that of other systems, occurs from the start of deformation, although these act only in a subordinate capacity.

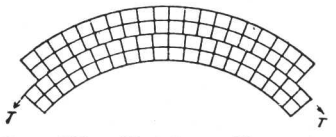

FIG. 199.—Sketch to Show the Process of Glide during Bending (608).

The conditions occurring on the internal separation planes are subjected to mathematical analysis in (609). It is shown there that the disorientation of a single atom in a series of atoms is unstable and that the atom must revert of its own accord to its position in the lattice. On the other hand, linear groups of disoriented atoms become stabilized. Consequently the resultant stresses remain even after the externally applied stress has been removed. A model illustrating very clearly the stability of these groups has already been shown in (610). The relationship between the two forces operating on irregular atoms (elastic energy exerted by one-half of the lattice on an atom belonging to it, but which has been forced out of equilibrium; energy which is present in the opposite half of the lattice and which changes periodically with the displacement) is assumed to be such that at least two stable equilibria are available for the displaced atoms. The transition from one position of equilibrium to the other proceeds by jumps when a given relative displacement of the lattice halves has been achieved. If the direction of stress is reversed, then in order to restore the original state it will be necessary to remove the load to a point at which the

deformation is smaller than that which is necessary to cause instability at that load. Thus, dependent upon the previous history, two different states of deformation can result from one and the same effective stress. This would explain elastic hysteresis in single crystals (cf. Section 55). The cause of the appearance and persistence of closed loops under alternating stress should be sought, not in the crystallographic mechanism of deformation, but in the mechanically reversible atomic movement between two adjacent stable positions (611).

The model described above has also been used to explain the low elastic after-effect of crystals. Thermal energy, and not the supply of elastic stress energy, is held to account for the jump from one state of equilibrium into another. The requisite amounts for overcoming the shear stress of the lattice are thus supplied locally in exactly the same way as was assumed in the theory of crystal flow by gliding (cf. Section 75).

According to a third group of hypotheses the cause of hardening must be sought in the atoms themselves. Control of the speed of solution, and the change which is produced in the colour of alloys by cold working, have been accounted for in this way (604). The circumstance that the lattice distortions which are revealed by X-ray photographs do not entirely correspond to the changes in the mechanical properties and the electrical resistance, and that the effect of hardening and recovery varies for different properties of metals of the same lattice type, has been put forward as evidence that a deformation of the electron shells of the atoms is the primary cause of the work hardening effects. These atomic deformations can be accompanied by slight disturbances of the crystal lattice, but they need not be so accompanied [(612), (613)]. Without denying the possibility of such atomic deformations, it should be pointed out that they ought rather to be regarded as a secondary effect of the primary lattice distortions (614).

It cannot be said at present which of these theories of work hardening will survive when our knowledge of the subject is more complete. It is, however, an advantage of the first group of hypotheses that they approach work hardening phenomena from the same angle as the equally unsolved problem of the low mechanical properties of crystals.

77. *The Theory of Recrystallization—Atomic Migration Plasticity*

The phenomena and principles of recrystallization (and crystal recovery) have been discussed in previous sections (49, 61–65 and

71). The process underlying this phenomenon is the *migration* of the atoms brought about by the increased thermal movement incidental to heat treatment. We shall discuss theories which enable us to understand the recrystallization temperature and the *shape* of the recrystallization diagrams. Then we shall describe a type of plasticity which, while it occurs with crystalline material, does not proceed in a regular crystallographic fashion but is also probably due to atomic migration.

There are two explanations for the existence of the temperature of recrystallization. The first, which applies to cubic crystals, relates to the thermal migration of atoms while also describing the diffusion processes (614*a*). A condition of atomic migration is that the energy of the atoms in question must be greater than a given limiting value (E), and this applies to that part of the atomic array which is represented by ($e^{-\frac{E}{kT}}$). With the aid of the specific atomic frequency (ν) both the number of migrations per second and the time required until all the atoms have migrated can be calculated. The deformed material is distinguished from the undeformed by an increase in energy (ΔE), which is characterized by the change in the specific resistance. The probability of migrations is thereby increased, since the quantity of energy to be produced by the thermal movement of the atoms is now only $E - \Delta E$; the time required for the migration of all atoms is reduced. An important prerequisite for the occurrence of recrystallization is the *unsymmetrical* distribution of energy accumulations in the deformed material, which otherwise would be indistinguishable from material at high temperature.

The points at which maximum accumulation of energy occurs determine the course of recrystallization. In order that the whole specimen may recrystallize, it is necessary that at several places all the atoms shall migrate during heating. The time of heating must therefore be stated in order that the temperature of recrystallization can be fixed. The connection established in this way, at a constant percentage of working, between recrystallization temperature $T_{R(\mathrm{abs})}$, time of heating t and atomic frequency ν, is as follows :

$$T_R = \frac{\text{const}}{\ln \nu t} \quad . \quad . \quad . \quad . \quad . \quad (77/1)$$

If, then, two related values of T_R and t are known, the heating period corresponding to another temperature of recrystallization can be calculated (thus an increase of T_R by 1 per cent. reduces

the time of heating by 35 per cent). This formula has been tested experimentally on various materials, and the results have confirmed theoretical expectations.

According to the second explanation the temperature of recrystallization is said to be that at which the speed of recrystallization changes abruptly (609). This phenomenon can be best explained with reference to the groups of disoriented atoms which occur in hardened crystals and which have already been described. The state of metastable equilibrium in which the disoriented atoms find themselves at the boundaries of the glide lamellæ increases with the number of atoms that are interlocked; the limiting energy required to overcome this equilibrium is therefore correspondingly great. If we heat a hardened crystal in which such interlocked atoms are dispersed, then, in accordance with Maxwell's Law of the distribution of energy, only a few interlocked atoms will have sufficient energy at low temperatures to free themselves from the bond. At such temperatures very long heating periods will be necessary to attain the final recrystallized state of equilibrium. If, however, the heat treatment supplies sufficient energy within a short time to a large number of interlocked atoms, then, as the mathematical analysis shows, all interlockings are dissolved simultaneously owing to the reduced stability. The temperature at which this occurs in a short time is the temperature of recrystallization.[1]

The shape of the *recrystallization diagrams* [coarse grain size after low percentage of working and high annealing temperatures; fine grain size after heating at low temperature specimens which had been heavily worked (cf. Fig. 169)] was derived qualitatively from thermodynamic considerations which avoid the still unknown details of atomic processes (600). The atomic migrations which take place at a temperature above that of recrystallization increase in frequency with the growing confusion of the atomic arrangement which augments with the percentage of working (increased hardening). If, as a result of this migration, a number of atoms arrive in positions which are crystallographically suitable, they will remain in these positions for a much longer period: a crystal nucleus will form. This means that the frequency of the migrations will decisively influence the formation and subsequent growth of crystal nuclei. In the first place it will be observed that not every new grouping of atoms is capable of serving as a nucleus. For instance, if the

[1] However, it is difficult to reconcile with this explanation the fact that the temperature of recrystallization falls as the percentage of working increases, while the number of interlockings, far from being reduced, probably grows as hardening proceeds.

number of related atoms is too restricted and the fragment of crystal too small, its stability will not exceed that of the deformed material in the immediate vicinity. If the nucleus remains below a certain critical size it will disappear again, since its vapour pressure exceeds that of its surroundings. The problem is, therefore, to represent the vapour pressure of the basic material as a function of the percentage of working and of the temperature of annealing, and that of the newly formed nuclei as a function of size and temperature. From an equalization of the two we obtain the minimum size (r) of the stable nucleus as a function of the percentage of working [measured by the heat of recrystallization (δ) and temperature (T)]. The expression for r is as follows :

$$\frac{1}{r} = \frac{\delta(T_s - T)}{T_s} \cdot \frac{d}{2\sigma M} \quad . \quad . \quad . \quad . \quad (77/2)$$

in which T_s represents the melting point, d and σ the density and surface tension of the crystal, M the molecular weight of the vapour. The dependence of the nuclear size (r) upon δ and T which results from (77/2) agrees with the shape of the recrystallization diagrams.

The foregoing discussion has dealt with the average grain size of the recrystallized structure. Observations relating to the distribution of grain sizes will be found in (615). In (616) grain-size distribution has been calculated on the basis of an assumed constant frequency of nucleus formation and constant linear speed of growth. This distribution should be the same both for the cast and recrystallized structures, but apparently it does not entirely conform to actual experience. To assume a constant speed of nucleus formation is to simplify the problem unwarrantably, at least so far as recrystallization is concerned.

In connection with this discussion of the recrystallization of hardened crystalline materials, attention should also be drawn to another consequence of the atomic migration phenomena. There is a type of plasticity which accompanies recrystallization (and phase transformations) in the course of stressing, and which strictly speaking cannot be regarded as a movement due to crystallographic glide. On the other hand, it can easily be explained as a result of atomic migration, since under stress those migrations are naturally preferred which lead to stress relief or to deformation consistent with the stress. This type of plasticity has therefore been designated "*amorphous plasticity*" because migration is the mechanism by which an amorphous vitreous material deforms. In this way it may happen that at temperatures above recrystallization a recrystal-

lized material, which has been annealed and softened, will be stronger than work-hardened unannealed material in which vigorous migration takes place as heating proceeds (600). Experiments with tungsten coils (617) and with copper and aluminium wires (618) reveal, in fact, that pronounced flow accompanies recrystallization. In Fig. 200, by way of example, flow curves are shown which were obtained in a filament-stretching apparatus with hard and soft copper wires treated at 600° C.; in every case the hardened recrystallizing wire flows more readily than the one which has been previously annealed.

Similar results have also been obtained when investigating the

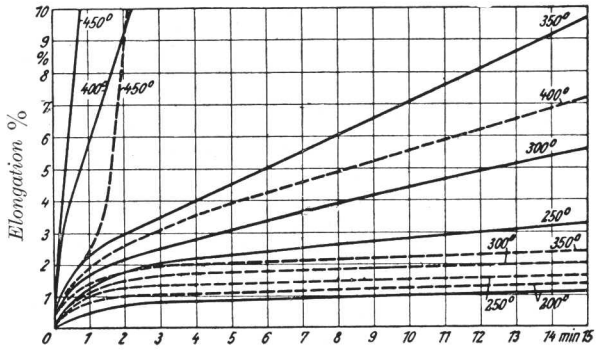

Fig. 200.—Flow Curves of Hard and Soft Copper Wires at Various Temperatures (618).

———— : Hard. – – – – : Soft.

" creep " strength of iron and nickel and of some of their alloys at elevated temperatures (619). The extensions in this case were not determined by mirror reading, but were compensated for by changing the temperature. It was again found that material which had been pre-heated was very much stronger (in terms of creep strength) at temperatures above the range of recrystallization. The technical significance of these facts is obvious. If the observed phenomenon is generally valid, then metals used within the temperature range in which recrystallization and recovery occur could in many cases be better employed in the heat-treated than in the cold-worked state.

In view of these facts it was natural to expect a reduction in flow resistance in cases of phase changes also. Here, too, atomic migration supplies the mechanism by which the lattice is reconstructed.

Detailed investigation of the γ–α phase change of nickel steel (30 per cent. nickel) has confirmed this expectation (620). If the phase change occurred while the wire specimen was being stressed, then extensions of more than 10 per cent. were observed to take place at the same time. Since the specimen had been merely cooled, it follows that in this case it cannot have been a question of migration of thermal origin. It is therefore the occurrence of active atomic migration, and not the manner in which this migration is brought about, which is the essential feature of the mechanical weakness.

CHAPTER IX

THE PROPERTIES OF POLYCRYSTALLINE TECHNICAL MATERIALS IN RELATION TO THE BEHAVIOUR OF THE SINGLE CRYSTAL

Having discussed the phenomena of the plastic deformation of single crystals, we saw in the previous chapter how far we still are from a satisfactory theoretical interpretation of the observed facts. The present and last chapter will be devoted to an examination of the problem—scientifically less impressive but technically very important—of the relationship between the properties of polycrystalline aggregates and the properties and arrangement of the individual grains (texture). An understanding of this relationship will enable us not only to explain the behaviour of aggregates, but also to estimate what properties can be obtained in the material under optimum conditions. A calculation of the properties of the material from the behaviour of the single crystal and the arrangement of the grains will be particularly successful if the effect of the grain boundaries does not make itself felt in the polycrystal.

In the first place it is the properties which are structure insensitive (cf. Section 60) for which crystalline behaviour and structure are the sole determining factors (*e.g.*, the elastic properties, thermal expansion). But even in the large group of plastic properties which are structure sensitive, we may expect to find a manifestation of polycrystalline behaviour which is at least qualitatively correct, owing to the directionality of these properties being frequently very marked. In this way we gain a clearer insight into a number of technological problems and so are enabled to make more effective use of the material. But in so far as the influence of the grain boundaries predominates, the method of approach outlined above becomes less applicable. Properties which are based on intercrystalline processes occurring at the grain boundaries, such as hot shortness caused by melting of a eutectic, intercrystalline disintegration due to corrosion—do not, of course, come within the scope of the present discussion.

Before dealing with the mathematical side of the problem, and before noting examples from the technology of metals, we will discuss the methods in use for determining the crystalline arrangement in polycrystalline material, and we will describe and trace to their origin the textures which are produced in metals by the various

methods of working. We have omitted rock structures from this discussion. These have been widely investigated in recent years, and the subject is treated exhaustively in the monographs [(621), (622)].

78. *Determination and Description of the Textures* (*see* 623)

In principle, the same methods are used for determining the distribution of orientations of the grains of a polycrystalline aggregate as for determining the orientation of single crystals (cf. Chapter IV). The superiority of the X-ray method has been clearly demonstrated, especially where fine-grained and intricate textures are involved, and it is this method which we propose to discuss almost exclusively.[1]

Supplementing the information contained in Chapter IV, we give below, briefly, the solution of the following two problems.

1. Determination of the orientation of crystal grains relative to a *direction* imposed by the shape or previous history of the specimen (*e.g.*, direction perpendicular to the cooling surface in cast material,[2] and to the longitudinal axis in drawn, rolled or recrystallized wires and extruded bars).

2. Determination of the texture relative to a *co-ordinate system of axes* suggested by shape or previous history (*e.g.*, the rolling, transverse and normal direction in sheets).

If, in the first case, one and the same lattice direction in each crystal grain coincides with the imposed direction (axis of the fibre), then the simplest type of crystallite arrangement is present and we obtain a simple fibre texture (625).[3] In this case a monochromatic X-ray diagram perpendicular to the working direction coincides with the diagram of a crystal which has been rotated about the relevant lattice direction. In the specimen all those crystalline positions are spatially distributed which appear successively as the crystal is rotated. The

[1] If a quick and rough estimate of the anisotropy of rolled sheet is required, the Chladni resonance figures can be used (624).

[2] Fig. 201 shows the structure of a technical casting. Several different zones can be clearly distinguished. At the outer edge, close to the wall of the die, there is a thin layer of fine-grained equiaxed crystals, which is followed by a fairly coarse-grained layer of columnar crystals, the longitudinal direction of which is perpendicular to the cooling surface. The interior of the bar is made up again of smaller crystals of irregular shape. Deviations from the random arrangement of the crystals are to be expected mainly in the columnar zone. The prevailing texture in this layer is known as the casting texture. When determining the texture by X-ray methods it is advisable that the test bars taken from the casting should have their axis parallel to the direction of growth of the crystals.

[3] Fibre—the name originates from the discovery of this type of texture in natural fibres (626).

interference patches are located on the layer lines, and it is from the distance of the latter that, knowing the crystal structure, and using formula (21/2a), the identity period along the fibre axis and the

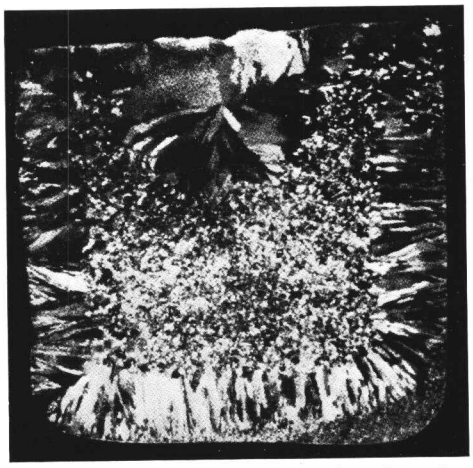

FIG. 201.—Cast Structure. Section through a Copper Ingot.

crystallographic nature of the texture can be determined. The nature of the fibre axis can be checked by examining the distribution of the interferences on the layer lines, which, as mentioned in Section 21, is entirely regular. Examples of a cast specimen and of

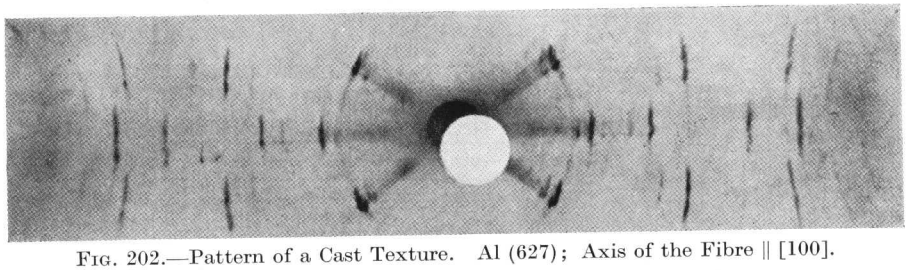

FIG. 202.—Pattern of a Cast Texture. Al (627); Axis of the Fibre || [100].

a recrystallized wire are shown in Figs. 202 and 203, which were obtained by irradiation perpendicular to the axis of the fibre. Fig. 204, a and b, reveals the presence of a so-called " double fibre texture " represented by the superimposition of two simple fibre textures with a fibre axis common to both. In this case there are

two groups of crystallites, each of which is characterized by a definite crystal direction parallel to the axis of the fibre.

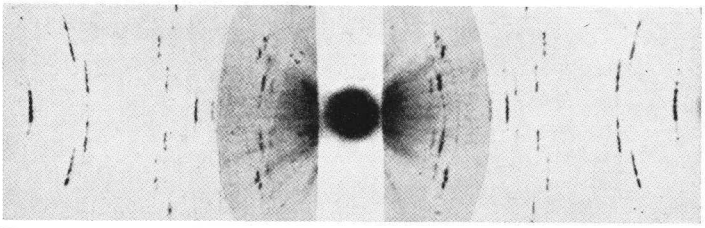

FIG. 203.—Fibre Pattern : Recrystallized Aluminium Wire (628); Axis of the Fibre ‖ [111].

As an example of the determination of the orientation of the crystallites in relation to a three-axial rectangular system of co-

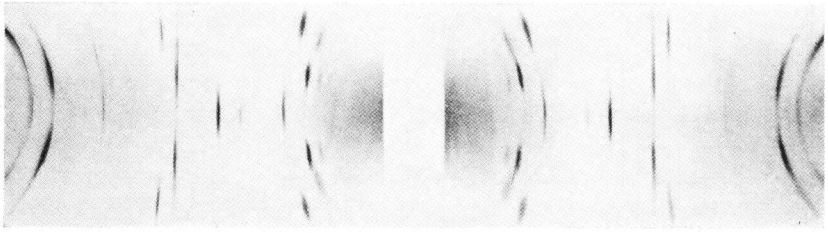

(*a*) Texture pattern.

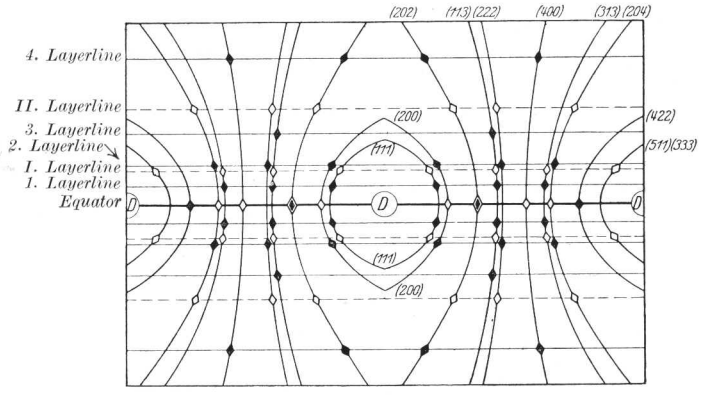

(*b*) Theoretical diagram of a double fibre-texture ; fibre axis ‖ [111] and ‖ [100]. The layer lines through the texture with Arabic numerals refer to [111], those with Roman numerals to [100].

FIG. 204 (*a*) and (*b*).—Drawing Texture : Cu (629).

ordinates, attention is drawn to the so-called pole figure method which was applied to metals for the first time in (631). This does not merely consist in giving the crystallographic directions which lie parallel to the three axes in the individual crystals, but also—and this is the main advantage—in a representation, characterized by pole figures of the more important crystal faces, of the whole distribution of orientations present in the specimen. In order to obtain these pole figures the interferences on the Debye–Scherrer circles are plotted in the stereographic representation of the normals of the reflecting planes (cf. Section 24, where this plot is shown for the Laue interferences). This method is used especially for defining the textures of sheets, and it is to such an application that the following remarks apply. If the distribution of orientations is to be fully accounted for, a single diagram taken approximately perpendicular to the plane of the sheet will by no means suffice. If the specimen is not moved, then reflections can be obtained only from those crystal planes which, according to Bragg's formula, are in an exact position to reflect. If therefore a complete picture is required, it will be necessary to irradiate the sheet obliquely in various directions to produce a series of photographs. It is preferable so to arrange the directions of radiation that they lie in the planes : sheet normal—rolling direction and sheet normal—transverse direction. In such oblique photographs the primary ray is no longer perpendicular to the rolling plane of the sheet, that is, to the projection plane. It will now be a question of transferring the interference positions of the oblique photographs to the stereographic projection, and so to a representation of the reflecting lattice planes. This is achieved by projecting the interferences first of all in the same way as the photographs which have been taken perpendicularly. The primary ray is then perpendicular to the projection plane. The plane of the sheet, however, does not coincide with the projection plane, as would be necessary for a uniform representation. On the other hand, the inclination of the sheet normals to the primary ray is known. For instance, if, in a photograph, the primary ray in the plane containing the sheet normal and the rolling direction has been inclined at an angle α to the sheet normal, then the sphere of reflection, which initially was projected perpendicularly, must be rotated about the transverse direction by the angle α. In this way the rolling plane will coincide with the projection plane, while the primary ray will impinge obliquely at angle α. Thus, a number of photographs can be evaluated and the results entered on the same stereographic projection. Finally, the points obtained are repro-

duced in accordance with the existing symmetry elements of the texture. With a view to a more exact definition, the density of distribution in the pole figure is estimated from the intensity of the reflections. The diagram is prepared either in terms of the different degrees of density (see Fig. 205) or by suitably shading the pole figure (see Fig. 206).

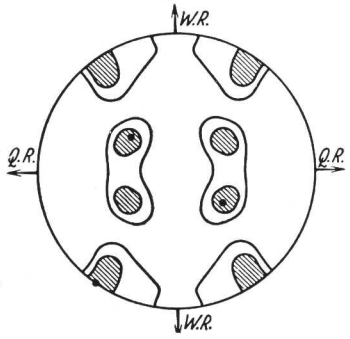

(*a*) Pole figure of the (100) plane.

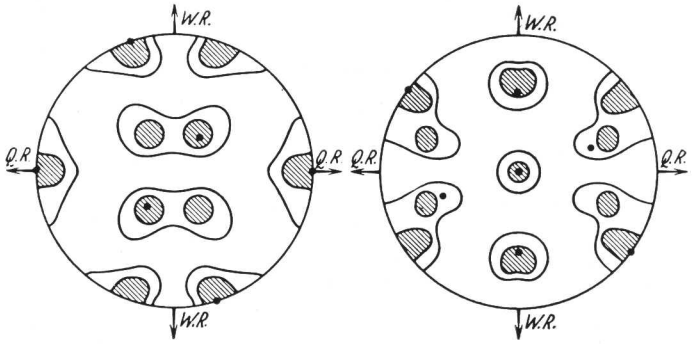

(*b*) Pole figure of the (111) plane. (*c*) Pole figure of the (110) plane.

FIG. 205 (*a*)–(*c*).—Rolling Texture of α-brass (632).
WR = direction of rolling. *QR* = transverse direction.

Table XXXI contains particulars of the casting textures of a series of metals and solid-solution alloys based on the *results of texture determinations* [in particular the determinations in (627)]. In the columnar zones there is a simple fibre texture : an important lattice direction coincides more or less in the fibre axis of all crystal dendrites. Zinc and cadmium are the only exceptions. Here a " circular " fibre texture is present (634); in all crystals the longitudinal direction is distinguished only in so far as it lies in the basal

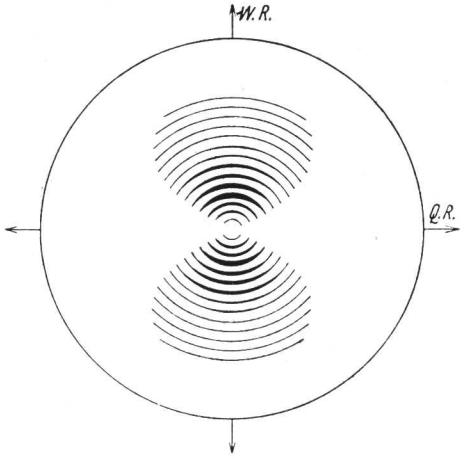

(*a*) Pole figure of the (0001) plane (basal).

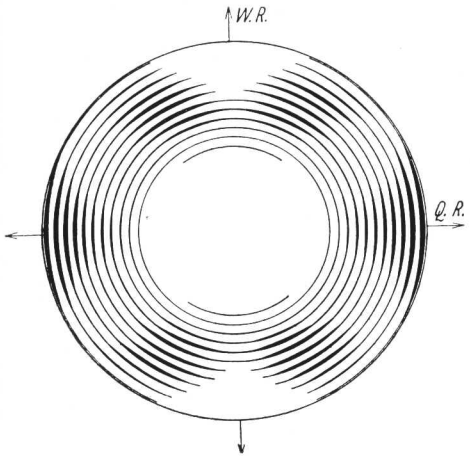

(*b*) Pole figure of the $(10\bar{1}0)$ plane (prism type I, order 1).

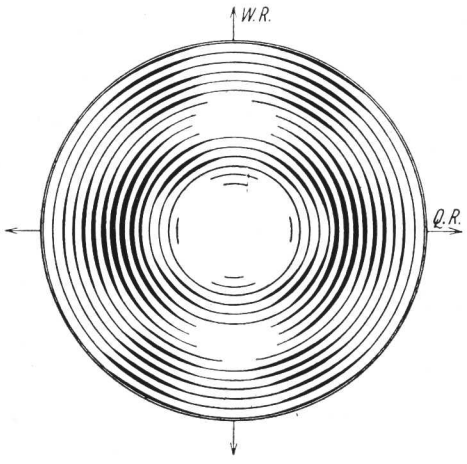

(*c*) Pole figure of the $(10\bar{1}1)$ plane (pyramid type I, order 1).

FIG. 206 (*a*)–(*c*).—Rolling Texture of Zinc (633).

WR = direction of rolling. QR = transverse direction.

plane; otherwise it presents a different direction from crystal to crystal.[1]

The deformation textures, which are distinguished according to the method of working (drawing textures, rolling textures, etc.), cannot as a rule be fully described by indicating the principal crystal orientations. With rolling textures the pole figure is usually employed. This indicates the degree of scattering, and so affords a better idea of the distribution of the crystal orientations present.

TABLE XXXI

Cast Textures

Metal.	Parallel to the longitudinal direction of the crystals.
Al, Cu, Ag, Au, Pb, α-Brass	[100]
α-Fe, β-Brass	[100]
β-Sn	[110]
Mg	[11$\bar{2}$0]
Zn, Cd	[0001] Perpendicular
Bi	[111]

But other refinements in the structure of the deformation textures must also be taken into account. They relate mainly to the inhomogeneity of the texture with regard to type and scatter in the different layers of the material. Where a double fibre structure is present it will also be necessary to indicate the frequency with which the individual crystal orientations occur. In Fig. 207 are found four diagrams which have been obtained from copper wire etched to different depths. It will be seen immediately from the varying

[1] Regular textures also occur, under suitable conditions, in metals which have been electrolytically deposited from aqueous solutions; they are simple fibre textures with the direction of the current flow serving as the fibre axis. A whole series of factors is responsible for the selection of this axis—solvents, ions in solution, amperage, the material of the cathode. For a summary of the observed textures, together with particulars of the working conditions, see (623).

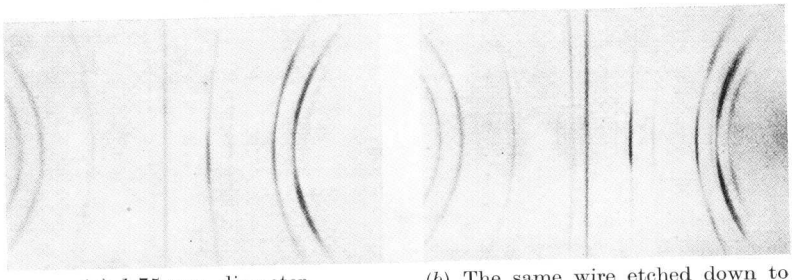

(*a*) 1·75 mm. diameter. (*b*) The same wire etched down to 1·3 mm.

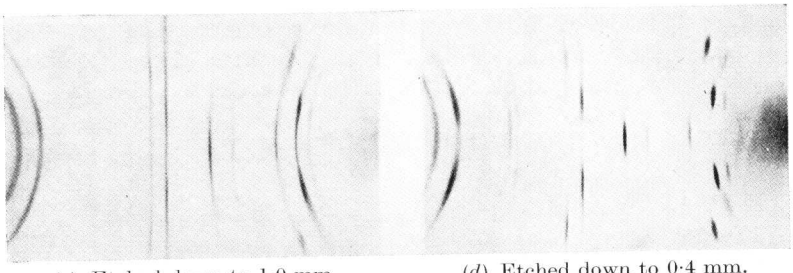

(*c*) Etched down to 1·0 mm. (*d*) Etched down to 0·4 mm.

FIG. 207 (*a*)–(*d*).—Texture Present in Different Layers of Drawn Copper Wire (629).

length of the interference arcs that the pattern is much sharper in the centre of the wire than in the peripheral zones. That this discrepancy in scatter is not due to differences in the thickness of the wire will be clear from Fig. 208, which illustrates drawn, unetched wire 0·05 mm. in diameter. In addition to the sharpness of the pattern, inhomogeneity affects also the texture (note the absence of symmetry in Figs. 207, *a*–*c*, and 208).

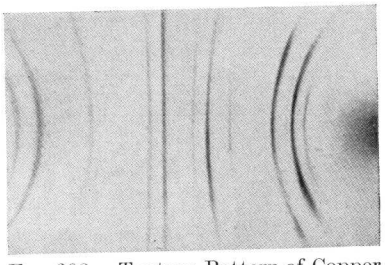

FIG. 208.—Texture Pattern of Copper Wire which has been Substantially Hard Drawn (629). Diameter : 0·05 mm.

The real drawing texture resulting from uni-axial tension can be described as follows in the case of cubic face-centred and probably also cubic body-centred metals : in the interior of the wire there is a normal fibre texture ; towards the exterior it merges gradually into

of the peripheral zones of the specimens even if not that of the interior. The particulars of the preferred orientations contained in Tables XXXII–XXXIV can therefore serve only as a first rough

TABLE XXXII

Drawing Textures

Metal.	Parallel to the axis of the wire.	
	1.	2.
Al	[111]	—
Cu, Au, Ni	[111]	[100]
Pd, Ag	[100]	[111]
α-Fe, W, Mo	[110]	—
Mg: drawn	(0001)	—
Mg: scraped	[10$\bar{1}$0]	—
Zn	(0001) Inclined at an angle of 18°	—

TABLE XXXIII

Compressive and Torsional Textures

Metal.	Compression. Parallel to the direction of compression.	Torsion. Parallel to the longitudinal direction.
Al, Cu	[110]	[111]
α-Fe	[111]	1. [110] 2. [112]
Mg	[0001]	—

approximation. In regard to Table XXXII (drawing textures) it should be observed that, despite the different method of fabrication, the same texture appears also in the interior of fracture cones of tensile bars, as well as in the interior of cold-rolled wires (copper, aluminium, β-brass). It would therefore appear as though the type of deformation employed, rather than the method of applying the force and the actual stress distribution, is mainly responsible for

the development of the structure [(638), (639); cf. also Section 80].

It is not easy to generalize regarding the textures which result from the heat treatment of cold-worked metals—recrystallization structures (cf. Sections 63 and 64). In this case, history, degree of purity and type of heat treatment profoundly influence the behaviour

TABLE XXXIV

Rolling Textures

Metal.	Parallel to the rolling	
	Direction.	Plane.
Al, Ag, α-Brass, (Pt)	[112]	(110)
Cu, Ni, (Au)	1. [112] 2. [111]	1. (110) 2. (112)
α-Fe, Mo	[110]	(001)
Mg	—	(0001)
Zn	[1120]	(0001)
	Inclined at an angle of 20°	Inclined at an angle of 20°
Cd	—	(0001) Inclined at an angle of 30°

of the material. Three main types of recrystallization can be distinguished in rolled sheets (640). First, the orientation of the new grains can be entirely random; secondly, a regular texture can appear at the onset of recrystallization, but it will be unstable, and a random distribution of orientations will be produced as treatment continues at higher temperatures; in the third case, the regular texture may persist at the highest annealing temperatures. As already mentioned, however, it is impossible to distribute the various metals accurately among these three groups. Aluminium, for instance, was at one time placed in the first group (640), but subsequent experiments revealed the presence of a regular recrystallization texture (641). In silver foil, which is representative of the second group, the recrystallization texture was found to disappear at 750° C. (642); but another type of silver foil retained the texture

even at high temperatures of heat treatment (632). Recrystallized copper foil, in particular, was considered by various authorities to belong unquestionably to the third group. In this case the very simple recrystallization position shown in Figs. 213 and 214 persists up to the highest temperatures. The hexagonal metals probably belong to this group also. The rolling texture of these metals has been observed always to correspond to the recrystallization texture [(645), (646)].

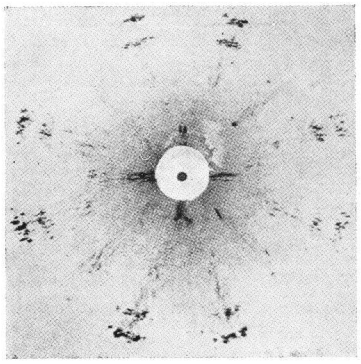

FIG. 213.—Texture Pattern of Recrystallized Copper Sheet (632). Cube Position.

The recrystallization textures of rolled sheets as defined by their main positions are shown in Table XXXV. The pole figures obtained with iron can be represented as three superimposed preferred positions, the first two occurring with nearly the same frequency, while the third is much more rare (647).

TABLE XXXV

Recrystallization Textures of Rolled Sheets

Metal.	Parallel to the rolling	
	Direction.	Plane.
Ag α-Brass Bronze (5% Sn)	[112]	(311)
Al Cu Ni Au	[100]	(001)
α-Iron	[110] [112] [110]	(001) (111) (112)

In annealed drawn wires the recrystallization texture at low temperatures is usually observed to be identical with that of the

drawing texture; the drawing texture still persists to some extent, however, in material which has been annealed at high temperatures. In pure aluminium wire the recrystallized texture is even more marked than the drawing texture (cf. Fig. 203). The recrystalliza-

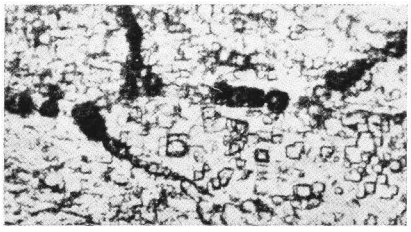

FIG. 214.—Etch Pits in Recrystallized Cu Sheet (643).

tion texture of copper wire which has been annealed at high temperatures differs from the drawing texture, being a simple fibre texture with [112] parallel to the direction of the wire.

79. *Behaviour under Strain of a Grain Embedded in a Polycrystalline Aggregate*

Before we discuss the development of textures we propose to examine in the present section, with reference to the formation of deformation textures, the behaviour under plastic strain of a single grain embedded in a polycrystalline aggregate, since the deformation of the aggregate also usually takes the form of a stretching of the individual grains and not of their displacement along the grain boundaries [cf. Fig. 215 and also (649)]. It is, of course, a fact that continuity on all sides with neighbouring crystals of different orientation results in considerable difference between the behaviour of the aggregate and that of the deformed, free, single crystal.

In order to make this difference clear, let us examine the case of a single crystal. If, for instance, two tin crystals are joined together along a short boundary, and if the crystals are then stretched, it will be noticed that the unjoined parts elongate with the typical formation of glide bands, while the region of the junction remains unchanged (650). It is obvious that the point of coalescence (the grain boundary) has a restrictive effect on elongation. If the stress were increased, the bi-crystal, too, would deform, but this would be accompanied by very substantial strains and distortions along the

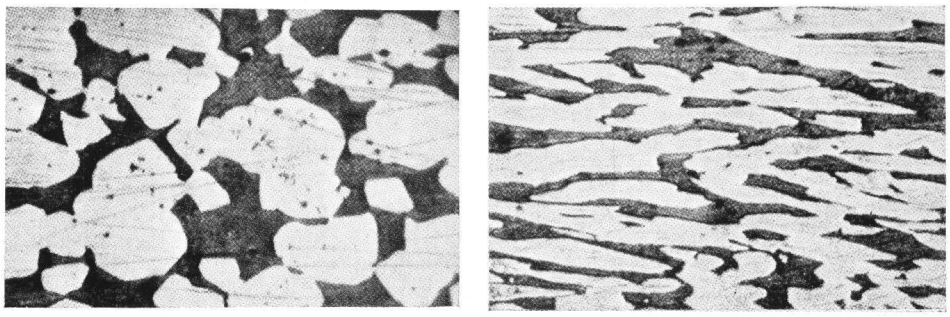

(*a*) (*b*)

(*a*) and (*b*) ($\alpha + \beta$)-brass before and after deformation (648).

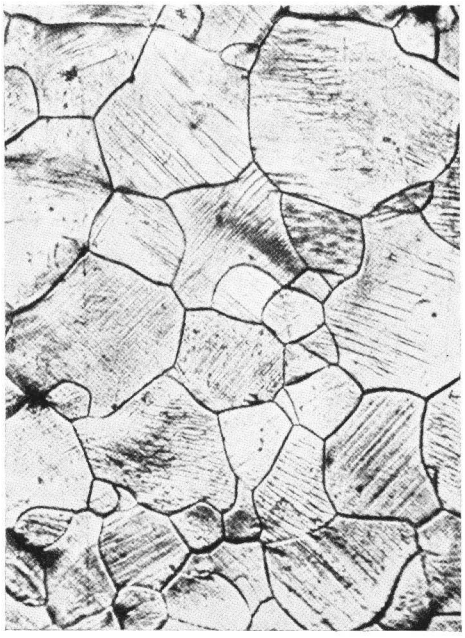

(*c*) Glide in a deformed Fe polycrystal (644).

FIG. 215 (*a*)–(*c*).—Grain Deformation Resulting from the Stretching of a Polycrystal.

grain boundary. These can develop to a point at which they cause grain boundaries to split, as has already been demonstrated in the

case of bi-crystals of bismuth. Indirectly the high strains along the grain boundaries are rendered visible by a greatly increased local capacity for recrystallization. Under annealing conditions which, in the elongated single crystal of tin, produce only a few large grains, the elongated bi-crystal changes into a fine crystalline structure.

These facts become intelligible when it is realized that the coalesced surface has to accommodate itself to the deformation of *both* crystals. This requires, however, that the crystals shall glide along the grain boundary, which would be impossible without overcoming the intercrystalline forces. If the stress is insufficiently

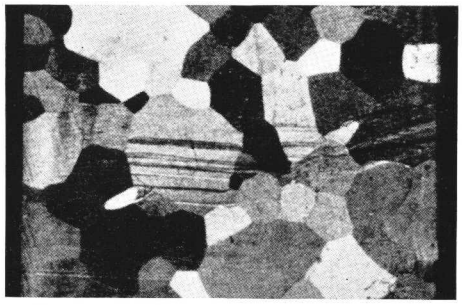

FIG. 216.—Slightly Bent Zn Sheet, with Chains of Deformation Twins (651).

raised, or if fracture takes place earlier, then the crystals deform in a way less suited to their inherent mode of deformation. Pronounced distortions of the crystal lattice occur, especially in the vicinity of the grain boundary, accompanied by such phenomena as greater work hardening and an increased capacity for recrystallization.

The grain boundary effect is even more considerable in polycrystalline aggregates than in bi-crystals. The single grain is much more restricted in its deformation by glide, being stressed along the whole of its surface by forces which distort it and impose upon it a very general modification of shape which cannot be achieved by simple glide alone. But if only a single glide plane is available, as in the case of the hexagonal metals, then the individual grains are but insufficiently equipped to bring about a general change in shape. In this case heavy additional distortions will be necessary, and in particular twinning, which results in greater hardening of polycrystalline aggregates than of the freely stretched single crystal for the same percentages of working. Fig. 216 shows by way of example

a coarse-grained zinc sheet which has been slightly bent, and which exhibits deformation twins in numerous grains. It should be noted that the twinning lamellæ often originate at the point of contact of three crystals and that connected chains form across the grain boundaries. Consequently, any portion of a grain boundary on which a deformation twin impinges is liable, owing to the very marked concentration of stress at this point, to give rise to another twin in a neighbouring crystal.

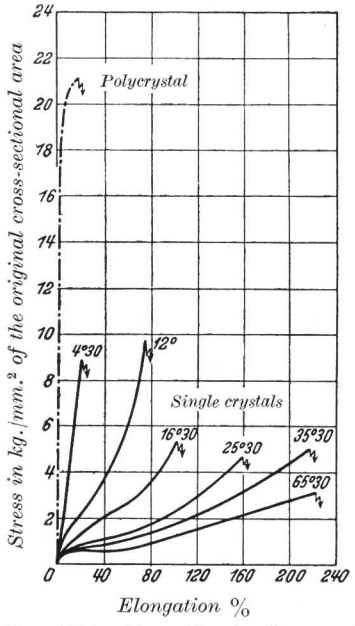

FIG. 217.—Stress–Strain Curves of Mg Crystals of Various Orientations, and of a Mg Polycrystal (655). The Initial Angles of the Basal Plane are Included for the Curves of the Single Crystals.

The position is different for cubic crystals, where there are many possibilities for glide. Face-centred crystals possess already twelve crystallographically equivalent octahedral glide systems. Consequently in their case deformation is by no means restricted to the system which is initially the most favourable, and multiple glide makes it much easier for the crystal to adapt itself to the imposed change in shape. Mathematical analysis has shown that any desired shape can be obtained if glide takes place simultaneously on five different glide systems (652). In such cases, therefore, much smaller differences may be expected in the hardening of single and polycrystals. This is confirmed by the stress–strain curves of single and polycrystals of magnesium and aluminium which are shown in Figs. 217 and 90*a* (page 121). It will be seen that, for the magnesium polycrystals, the stress applied is greatly increased and the ductility reduced compared with the single crystal; while for aluminium the stress–strain curve of the polycrystal falls within the limits of the curves for the single crystal [(653), (654)].

A similar contrast between the behaviour of hexagonal and cubic metals is observed under dynamic stressing. While with magnesium polycrystals subjected to alternating torsional stress fracture starts as a rule along the grain boundaries (high stress

concentration caused by restricted ductility), with aluminium polycrystals the course of fracture is mainly transcrystalline [(656), (657), (658)].

The interaction between the crystals becomes increasingly important with decreasing grain size. Similarly, work hardening is observed to increase with decreasing grain size for the same amount of deformation (659). Hardness, too, increases with decreasing grain size (cf. 660). It is possible that the experiments which revealed an exceptional increase in the tensile strength of zinc sheets with increasing fineness of the grain admit of a similar explanation (661). This would mean that, despite the low temperature of the test (−185° C.), the results could be interpreted in terms of tensile hardening dependent upon grain size (compare with this the very different interpretation in Section 75).

80. *On the Origin of Textures*

The cast structure usually results from the location of the longitudinal axes of the columnar crystals at right angles to the cooling surface (wall of the mould). This also holds for relatively intricate moulds (662). A principle of selection which explains the columnar arrangement and the existence of an orderly structure in terms of geometry and crystallography can be obtained from Fig. 16 (page 28). Having regard to what has already been said in Section 13, the fibre axis which corresponds to the longitudinal direction of the columnar crystals should be identified with the direction of maximum speed of growth in the crystal. According to this conception the crystal directions given in Table XXXI must also represent the directions of maximum speed of crystallization.[1]

The reorientations experienced by the individual grains in the course of working are closely related to deformation textures. This has been strikingly confirmed by the interpretation of the deformation textures of hexagonal metals, and by the great difference in behaviour of zinc and cadmium on the one hand and magnesium on the other (663). The mechanism which is mainly responsible for the change of shape, namely basal glide, makes the basal plane approach a position parallel to the direction of deformation. In the case of magnesium it is impossible for twinning to follow gliding, since with the basal plane in the above position, twinning would be accompanied by a contraction in the tensile or rolling direction

[1] It is probable that the electrolytic textures owe their origin to a similar selection in growth.

(cf. Section 31, and especially Section 39). The process of stretching therefore results mainly in primal basal glide. The most frequent end position is one in which the basal plane lies in the tensile direction or rolling plane. The compression texture observed in magnesium is also what would be expected from the behaviour of the single crystal. In zinc the formation is somewhat more complicated. Tensile tests on single crystals have already shown that in this case primary basal glide is followed by mechanical twinning, which, unlike the case of magnesium, results in a lengthening of the crystal. The angle of inclination between the basal plane and direction of tension at which the new type of deformation becomes effective is between 8° and 16° at room temperature. Twinning brings the basal plane into a position about 60° to the tensile direction, where it is again favourably oriented for further glide, with the result that very considerable secondary glide takes place in the twin lamellæ. It is in the texture of rolled sheet that all the stages of this tensile deformation are present simultaneously (cf. Fig. 206*a*). The most frequent final position of the basal plane is found experimentally to be about 10–20° to the direction of deformation (rolling direction). In many grains, however, the basal planes are inclined at steeper angles, since twinning leads continually to a reorientation of the basal plane followed by further gliding. The absence of basal-plane normals in the plane containing the sheet normal and transverse direction is readily explained by the fact that grains which are oriented in this way cannot undergo any lengthening in the rolling direction, and so must be brought, initially by twinning, into an orientation which is more suitable for subsequent deformation.[1]

Difficulties often arise, however, when such a direct interpretation of polycrystalline textures is attempted for cubic metals. For instance, the tensile and drawing structure of cubic face-centred metals is a double fibre texture having the [111] and [100] directions parallel to the tensile direction. In the case of stretched single crystals the [112] direction finally coincides with this direction. In spite of numerous attempts, no one has yet quite succeeded in deducing, quantitatively, the orientations of the crystallites in deformed components. The various assumptions can be grouped as follows: a mechanical principle assumes that the deformation texture is characterized by maximum strength. As cold working

[1] In heavily rolled sheets of a 99 per cent. zinc alloy a further restricted area has been found about the rolling direction in addition to the areas already described for the hexagonal axis. The stability of this orientation is understandable, since neither by gliding nor by twinning can deformation be achieved in the rolling process (664).

proceeds, the crystal elements are supposed to rotate gradually into an end position which is symmetrical to the main directions of deformation, and which requires a (relatively) maximum of externally applied force if further deformation is to take place (665). However, as is shown by the dependence of the yield point on orientation, the general validity of this principle is not proven. The other hypotheses relate primarily to the behaviour of the individual grain in the polycrystalline aggregate which is being deformed in tension. In (666) the point of departure is the assumption that the glide planes are bent about an axis perpendicular to the direction of gliding (direction of curvature). The reorientation of the grain embedded in the polycrystalline aggregate is said to correspond to this bending. The final position of the lattice is attained by activating two glide systems at the most. Although in certain cases the correct textures can be inferred from these assumptions, this is not always so. In particular, the case of the rolling textures of cubic metals remains unexplained.

The third group of hypotheses deals with the differences in the behaviour of extended free crystals and crystals in an aggregate which were described in the previous section. In (667) it is assumed that, if the imposed general change in shape is to be explained satisfactorily, then all the crystallographically equivalent glide systems must become active within the extended grain in the polycrystal. It has been found that, if certain allowances are made in regard to capacity for glide of glide planes and directions, the observed textures can be conceived as stable final configurations. The employment of three glide systems for the deformation of grains in cubic metals is indicated in (668) and discussed in detail in (669). Since the glide system which operates is determined by the shear stress, the magnitude of the prevailing shear stress is utilized for selecting the effective glide elements, and that final orientation is determined which, for the prescribed deformation, remains resistant to glide in the three most favourable glide systems. It was along these lines that the well-known drawing and compression textures of cubic metals could be interpreted. The main position of the rolling textures appears as a superimposition of compression and drawing textures. It is revealed as that final orientation which remains stable when compressed parallel to the sheet normals and elongated in the direction of rolling.

Another point of view from which to interpret the deformation textures is provided by the observation that different types of stress giving identical deformation yield identical textures. We have

seen, for instance, that the cold rolling of wires (copper and aluminium) produces the same texture as pulling or drawing them (639), and that steel sheet drawn through flat dies exhibits the same texture as rolled sheet (638). This emphasizes clearly the importance of the change in shape for the development of the textures. It therefore appears that the symmetry of the direction of flow in the metal is a more influential factor than the symmetry of the applied forces.[1] We again observe the importance of the direction of flow in the case of the inhomogeneous texture of wires drawn in one direction. In the centre of the wire the direction of flow coincides with the direction of drawing. Here the undisturbed texture can develop. At the surface, on the other hand, the material is compelled by the conical die wall to flow towards the centre. The axes of the crystals are rotated relative to the longitudinal direction, the amount of the rotation corresponding roughly to the taper of the die.

We are still unable to account fully for the origin of recrystallization textures—which, as already stated, are largely influenced by the conditions under which they are produced. However, it is reasonable to suppose [cf. especially (670)] that, also in the case of deformed polycrystals, recrystallization proceeds in two phases, namely by nuclear formation and grain growth—a mechanism which can be inferred especially from experiments which have been carried out with deformed aluminium crystals (cf. Section 63 and also 77). Opposed to this view is the " single-phase " conception of the recrystallization process (671). According to this theory those parts of the lattice which are least deformed serve as nuclei for the new lattice; removal of the distortions which are present in the deformed state enables these nuclei to grow. Consequently, over moderately large lattice areas only a *single* lattice orientation is present—although in various conditions, according to the number of distortions (" *Gehalt an Verhakungen* ").

81. *Calculation of the Properties of Quasi-isotropic Polycrystalline Aggregates*

As already pointed out, effective calculation of the behaviour of crystal aggregates, based on the behaviour of the single crystal,

[1] In this connection it might be possible to interpret the deformation textures by determining the stable end positions of the lattice at which those three glide systems become active which give maximum extensions in the preferred directions of flow for the same amount of glide (minimum energy of deformation). Since for small amounts of glide the strain is obtained by dividing the amount of glide by the same divisor ($\sin\chi \cos\lambda$) as when calculating the shear stress from the tensile stress (see Section 26), the same choice of glide systems becomes available as under the condition of maximum shear stress.

should be possible especially for those properties for which grain boundary interferences can be disregarded.

Hitherto, calculations have been carried out principally for the quasi-isotropic polycrystal (random orientation). Common to all determinations of average values is the assumption that the grains are large with respect to the range of the binding forces, but small in relation to the dimensions of the specimens, and that they completely occupy the space.

For the *elastic properties* this averaging (*Mittelung*) was first undertaken in (672) at a time when experimental material for testing the formula was scarce. The adhesion of the grains during elastic deformation is assured if one assumes that the stresses and strains are continuous across the grain boundaries. The averaging of the stress components (equation 7/1) for the polycrystal of random orientation is then based on the mean value of the elastic parameters C_{ik}. Integration of these expressions over the total range of orientation gives the elastic parameters of the polycrystal (in accordance with the system in Section 8) from which the moduli of elasticity and torsion are then derived.

It has been shown in (673), as the result of tests carried out on a number of metals, that while this method of calculation yields fairly accurate values for crystal material which is slightly anisotropic, the margin of error increases with increasing anisotropy. This is attributed to the conditions which exist at grain boundaries. Since the principle of action and reaction requires that the three stress components perpendicular to the boundary plane in adjacent crystals shall be equal to each other, it will usually be possible for only three, and not for all six, elastic deformations to be equivalent to each other. Very great difficulties are encountered when arriving at averages under the new limiting conditions. It becomes necessary to assume a special lamellar type of structure in the polycrystal. Such calculations yield a noticeably closer approximation to the values of the moduli as determined experimentally. The first process mentioned above is found to be an approximation where only slight anisotropy exists.

Underlying all calculations of averages is the assumption of a state of uniform stress in all grains (674). The new calculation proceeds along analogous lines (672), except that in accordance with the changed assumption the average is reached by way of S_{ik} [equation (7/2)]. This method of calculation yields values which are persistently lower than the observed results.

Finally, in (675) averaging is performed by integrating over the

whole range of orientation the expressions for the moduli of elasticity and torsion, as given by the theory of crystal elasticity, for a specimen taken in any desired direction relative to the crystallographic axes [formulas (10/1, 2) and (10/4, 5)]. Special limiting conditions governing the constancy of the components of stress or deformation become superfluous at the grain boundaries. This is justified because the cohesion of the grains is assured by the distortions which take place in the outer layers. This can, in fact, be directly observed in the case of the much larger stresses which lead to plastic deformation. Integration over the total range of orientation (corresponding to the random texture of the polycrystal) results in finite expressions for the moduli of hexagonal crystals, and in rapidly converging series for those of cubic and tetragonal crystals (676). This method of averaging reproduces the observed facts with at least the same degree of accuracy as that described in (673). A statistical comparison with the results obtained in practice will be found below in Table XXXVI (678).

TABLE XXXVI

Calculated and Experimentally Determined Properties of Polycrystalline Metals (Random Orientation)

Metal.	Modulus of elasticity, kg./mm.².		Modulus of shear, kg./mm.².		Thermal expansion, 10^{-6}.		Specific electrical resistance, 10^{-6} Ω/cm.		
	Calculated.[1]	Observed.[2]	Calculated.	Observed.[2]	20–100° C. calculated.	0–100° C. observed.[3]	Calculated (81/3).	Calculated (81/2).	Observed.[3]
Aluminium	7,170	7,200	2,660	2,700					
Copper	11,950	12,100	4,280	4,400					
Silver	7,500	8,000	2,640	2,700					
Gold	7,750	8,100	2,650	2,800					
α-Brass (72% Cu)	10,500	10,200	3,550	4,100					
α-Iron	20,700	21,400	7,770	8,400					
Magnesium	4,510	4,500	1,770	1,800	25·9	26·0	4·29	4·32	4·4
Zinc	10,040	10,000	3,620	3,700	30·7	30·0	5·89	5·91	6·0
Cadmium	6,110	5,100	2,130	2,200	31·8	31·6	7·30	7·37	7·4
β-Tin	4,480	4,650	1,570	1,700	20·5[4]	23·0	11·0	11·4	11·1

Isotropic.

[1] All calculations based on the properties of crystals recorded in Tables XVIII and XX.
[2] According to Landolt, Bornstein, Roth and Scheel, *Physico-chemical Tables*, 5th edition.
[3] According to F. Kohlrausch, *Manual of Practical Physics*, 16th edition.
[4] At approximately 20° C.

In this context, mention may be made of Poisson's equation (cf. Section 9). It has been found that when applying the averaging process according to (672), the validity of the Cauchy relations for